Observations of 2–4 day inertia-gravity waves from the equatorial troposphere to the *F* region during the sudden stratospheric warming event of 2009

S. Sathishkumar[1] and S. Sridharan[2]

Received 23 August 2011; revised 30 September 2011; accepted 17 October 2011; published 17 December 2011.

[1] We have observed strong 2–4 day wave activity in the *F* region peak critical frequency (f_oF_2) at 7.5°N obtained from GPS radio occultation measurements of the Constellation Observing System for Meteorology, Ionosphere, and Climate (COSMIC) satellites and the horizontal component of geomagnetic field variations over Tirunelveli (8.7°N, 77.8°E, 1.75°N dip angle) during the sudden stratospheric warming (SSW) event of 2009. A similar wave is observed strongly in the meridional winds observed by the MF radar at Tirunelveli. The meridional winds at 9°N and the equator obtained from ERA-Interim, which is the latest global atmospheric reanalysis produced by the European Centre for Medium-Range Weather Forecasts, shows clearly the 2–4 day wave, propagating eastward with zonal wave number 6 over the central and eastern Pacific, both before and during the SSW event, and over the Indian sector during the SSW event only. The potential vorticity (PV) intrusion at 200 hPa to lower latitudes is near the central Pacific before the onset of the SSW event. However, during the SSW event, the PV intrusion is observed more strongly near the Indian sector in addition to the weaker intrusion near the central Pacific. It clearly indicates the Rossby wave propagation to equatorial latitudes in the form of PV intrusion, and it selectively enhances the periodicities generated owing to equatorial convective heating. These waves could propagate to upper heights and cause variations in the mesosphere-thermosphere-ionosphere system.

Citation: Sathishkumar, S., and S. Sridharan (2011), Observations of 2–4 day inertia-gravity waves from the equatorial troposphere to the *F* region during the sudden stratospheric warming event of 2009, *J. Geophys. Res.*, *116*, A12320, doi:10.1029/2011JA017096.

1. Introduction

[2] The F layer electron density profile presents considerable day-to-day variability, even during undisturbed conditions, and this variability is still one of the less understood aspects of the physics of the ionosphere. The day to day variations of geomagnetic field, which reflect the *E* region current system variabilities has been still an outstanding problem. Variabilities of up to 20% daytime *F* region maximum electron density cannot be associated with solar drivers [*Rishbeth and Mendillo*, 2001]. The variabilities are mostly caused by the gravity waves and planetary waves of lower atmospheric origin during the period of low solar activity either directly by modification of thermospheric winds by these waves or indirectly through the *E* region dynamo. The propagation of waves into the ionosphere may play an important role in this day-to-day ionospheric variability [*Fagundes et al.*, 2005]. The ionospheric variability often shows planetary wave periods (e.g., quasi-2 day, 5–7 day, 9–15 day, etc.) [*Laštovička and Pancheva*, 1991; *Chen*, 1992; *Altadill and Apostolov*, 2001; *Xiong et al.*, 2006]. Owing to the extended solar minimum since 2008, the level of geomagnetic activity has been very low. At quiet times during the day time, the *E* region dynamo effects are stronger and electric field changes in the *E* region propagate efficiently into F region heights. There are numerous observations of gravity waves at F_2 layer heights, dating even back to *Munro* [1948]. Recent studies have shown the large perturbations of ion temperature, ion drift, and total electron density during stratospheric sudden warming (SSW) events [*Goncharenko and Zhang*, 2008; *Chau et al.*, 2009]. Because a SSW is caused by the rapid growth of planetary waves [*Matsuno*, 1971], the observed ionospheric variability during and immediately after the SSW event could be related to these waves.

[3] Though SSW is a high-latitude phenomenon, the circulation changes associated with it could couple high and low latitudes from troposphere to ionosphere together. The SSW event is caused by an anomalous growth of Rossby waves which, owing to refractive index property, refract toward equator and cause potential vorticity advection, which subsequently enhance vertical motion and convection at low latitudes. The convective heating could generate equatorial

[1]Equatorial Geophysical Research Laboratory, Indian Institute of Geomagnetism, Tirunelveli, India.
[2]National Atmospheric Research Laboratory, Gadanki, India.

0148-0227/11/2011JA017096

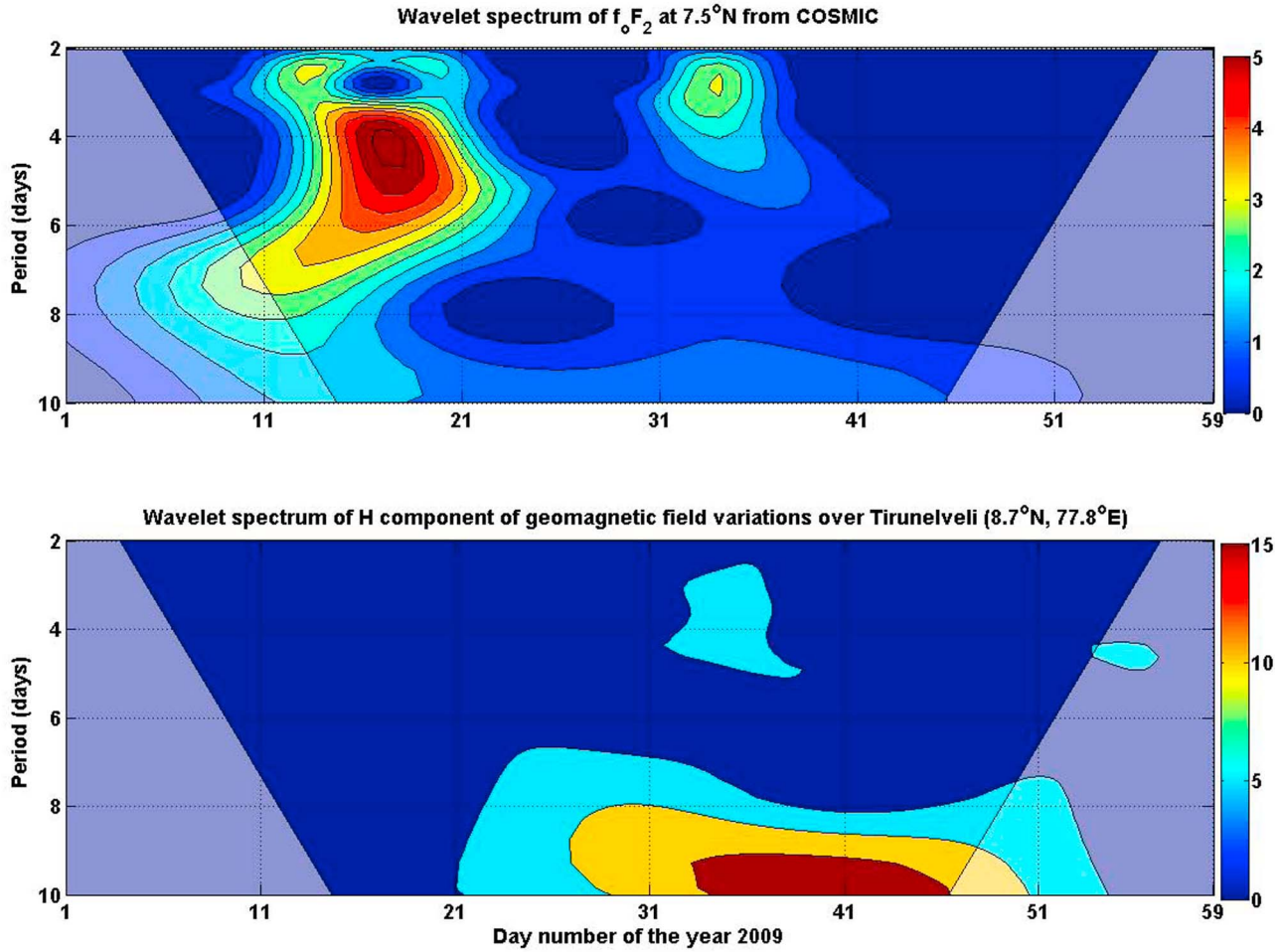

Figure 1. Wavelet spectra of (top) COSMIC GPS f_oF_2 variations at 7.5°N (0–10°N) and (bottom) horizontal component of geomagnetic field variations over Tirunelveli (8.7°N, 77.8°E).

waves, which can propagate to upper heights and may contribute to the variabilities of equatorial and low-latitude mesosphere-thermosphere-ionosphere system. *Charney* [1963] earlier proposed the possible forcing of the tropical atmosphere from higher latitudes. *Webster and Holton* [1982] showed that extratropical Rossby waves could propagate into the Tropics in regions of westerly winds in the upper troposphere. *Hoskins and Yang* [2000] showed that the equatorial response to high-latitude forcing is due to a direct projection of the forcing onto equatorially trapped waves and the Rossby-gravity wave dominates for the ~4 day period forcing and Rossby waves are found for the ~8 day period forcing. For the mesosphere-lower thermosphere-ionosphere region, little has been reported concerning the 2–4 day periodicities.

[4] In the present work, we have examined 2–4 day periodicities in the equatorial troposphere to ionosphere using COSMIC GPS F region peak critical frequency (f_oF_2), horizontal component of geomagnetic field and MF radar winds over Tirunelveli (8.7°N, 77.8°E), Rayleigh lidar and radiosonde observations at Gadanki (13.5°N, 79.2°E), ERA-Interim data sets, which is the latest global atmospheric reanalysis produced by the European Centre for Medium-Range Weather Forecasts (ECMWF), and outgoing longwave radiation.

2. Data Sets

2.1. COSMIC GPS f_oF_2

[5] The Constellation Observing System for Meteorology, Ionosphere, and Climate (COSMIC) is a joint Taiwan–United States mission, which launched six low Earth-orbiting (LEO) microsatellites in early 2006. Each spacecraft utilizes four GPS antennas: two occultation antennas for 50 Hz tracking for atmospheric profiling in an open-loop (OL) mode and two single patch antennas for 1 Hz tracking for precise orbit determination (POD) and ionospheric profiling [*Rocken et al.*, 2000; *Schreiner et al.*, 2007]. The ionospheric parameters f_oF_2 and h_mF_2 employed in this study were retrieved by the COSMIC satellite using the radio occultation inversion technique. The f_oF_2 data were downloaded from the Website http://cosmic.io.cosmic.ucar.edu/cdaac/. In the present study, the f_oF_2 data, averaged for the latitudes between 5°N and 10°N are used.

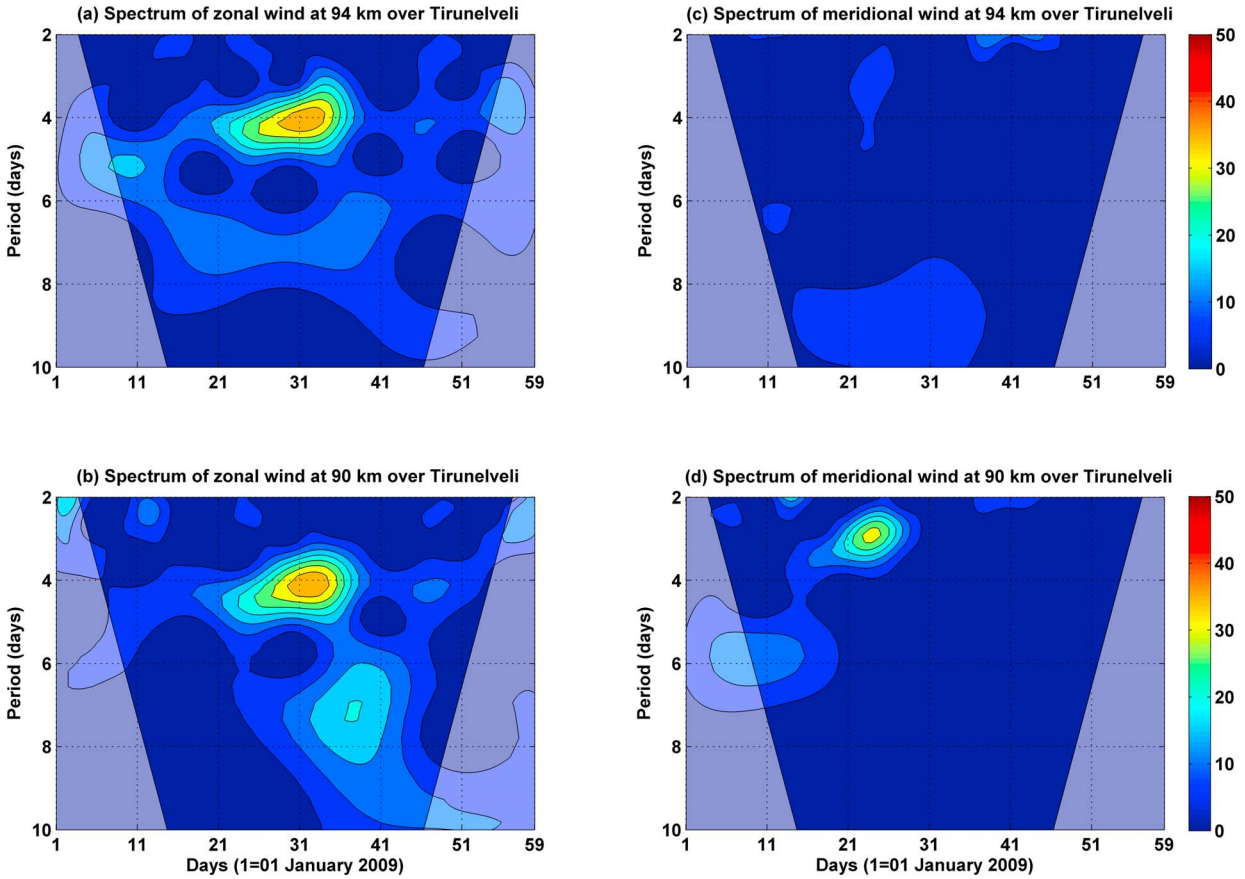

Figure 2. Wavelet spectra of zonal and meridional winds (MF radar) at (top) 94 km and (bottom) 90 km over Tirunelveli.

2.2. MF Radar Wind and Delta H Observations at Tirunelveli

[6] The variations in the three components of the geomagnetic field have been recorded by a network of magnetic observatories of Indian Institute of Geomagnetism located from the magnetic equator to the northernmost Indian latitudes. As the Tirunelveli (8.7°N, 77.8°E, 1.75°N, dip) is close to geomagnetic equator, geomagnetic field is nearly horizontal. In this study, the horizontal component of geomagnetic field variations are used to infer planetary/gravity wave variabilities. The 1.98 MHz medium frequency radar at Tirunelveli has been installed and operated by the Indian Institute of Geomagnetism since November 1992 [*Rajaram and Gurubaran*, 1998]. It provides horizontal wind information in the altitude region 68–98 km for every 2 km height interval and 2 min time interval. The pulse width of 30 μs limits the height resolution to around 4.5 km, so that there is a certain overlap of adjacent height gates. The raw winds for every 2 min are averaged for every hour and are used for further analysis. The daily averaged zonal and meridional wind data for the period January–February 2009 are considered in the present study.

2.3. GPS Radiosonde and Rayleigh Lidar Observations at Gadanki

[7] Meisei GPS radiosondes have been launched using TOTEX balloons almost daily at Gadanki since July 2006 around 12:00 GMT (17:30 LST). The atmospheric parameters, namely, pressure, temperature, relative humidity, horizontal wind magnitude and its direction are collected with a height resolution of 5–10 m (sampled at 1 s intervals). The horizontal winds, temperature, and humidity are measured with an accuracy of 0.15 m/s, 0.5 K, and 2%, respectively [*Debashis Nath et al.*, 2009]. Quality checks have been applied to remove outliers in the data sets [*Tsuda et al.*, 2006], which may arise owing to random motion of the balloon. The entire data set has been interpolated to 100 m and used for the present work. The Rayleigh lidar system at Gadanki transmits its second harmonic output at a wavelength of 532 nm vertically upward and the backscattered photons are collected with a 75 cm diameter Newtonian telescope, are counted sequentially, using a multichannel scaling averager, into successive range bins of equivalent width of 300 m. The Rayleigh lidar technique is based on the assumption that in the absence of aerosol (i.e., above 30 km altitude), the backscattering photons is directly proportional to molecular density. Using a half-hour integrated photon counts profiles, relative density profiles are obtained by correcting for range-squared dependence and normalizing the backscatter profile at an altitude of 40 km. An absolute temperature profile is derived using equations of ideal gas law and hydrostatic equilibrium [*Hauchecorne and Chanin*, 1980] in the altitude region 30 to 90 km.

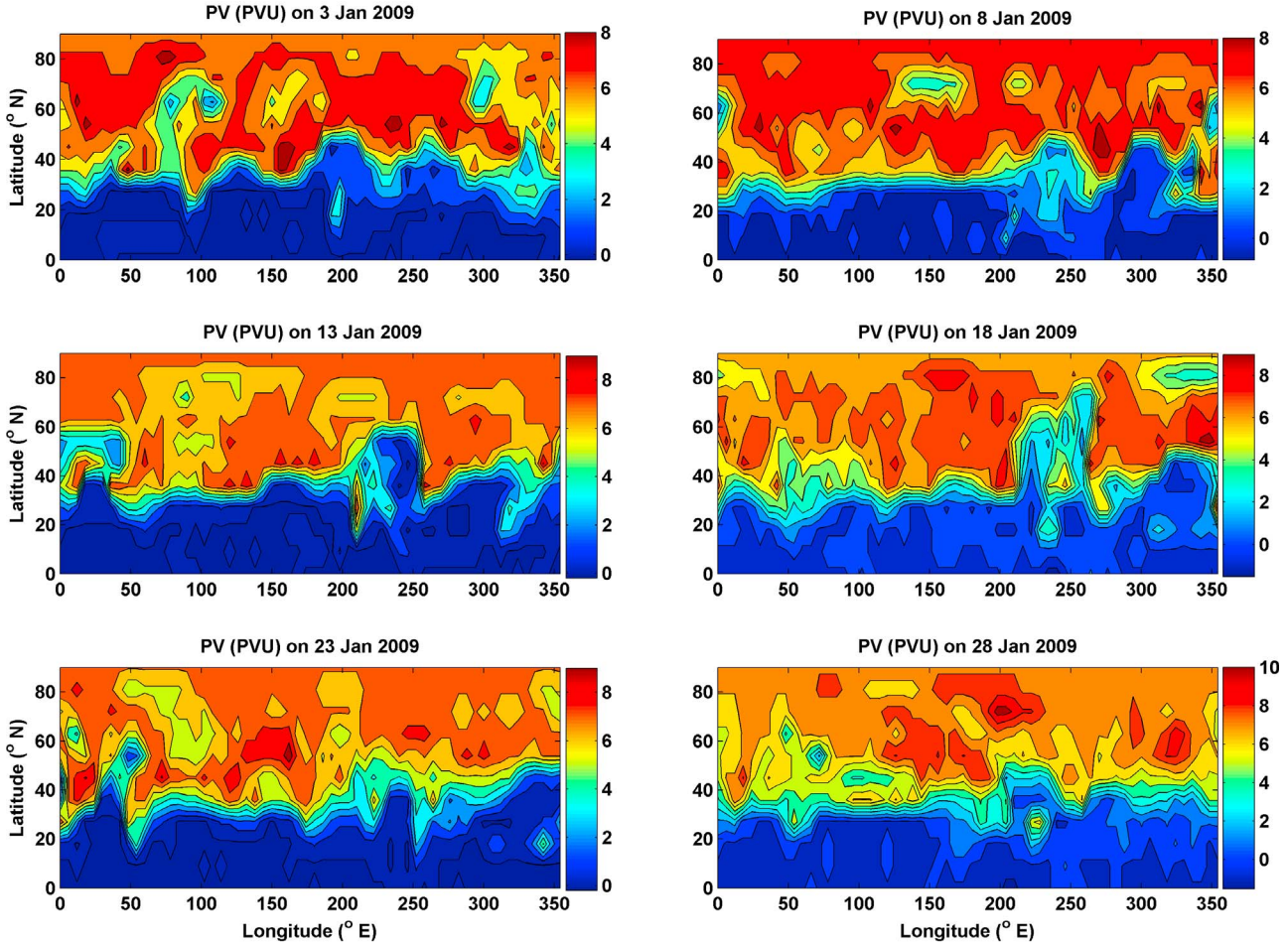

Figure 3. Latitude-longitude map of isentropic potential vorticity ($\times 10^{-6}$ K m^2 kg^{-1} s^{-1}) at 200 hPa on a few selected days of January 2009.

2.4. ERA-Interim and NOAA Outgoing Longwave Radiation

[8] The information about prevailing meteorological and dynamical conditions in the stratosphere is addressed using ERA-Interim reanalysis. It is archived on the ECMWF (European Centre for Medium-Range Weather Forecasts) Web site: http://data-portal.ecmwf.int/data/d/interim_daily/. The dynamical variables such as wind and temperature components are extracted from ECMWF/ERA-Interim with the grid size of 1.5° × 1.5° from 1000 to 1 hPa pressure levels [*Uppala et al.*, 2005]. The daily interpolated (2.5° × 2.5°) outgoing longwave radiation (OLR) data archived from the NOAA satellite are used as a proxy for the tropical deep convection. Lower values of OLR correspond to more enhanced convective activity. For example, the OLR which is less than 240 W/m^2 is a general indicator of precipitation in the tropics [*Lau and Chan*, 1983].

3. Results

[9] The wavelet analysis is applied to horizontal component of geomagnetic field variations over Tirunelveli and zonal mean GPS f_oF_2 observations at 7.5°N. The wavelet analysis is a common tool for analyzing localized variations of power within a time series. By decomposing a time series into time-frequency space, it is possible to determine both the dominant modes of variability and how those modes vary in time [*Daubechies*, 1992]. For the present study, we use Morlet wavelet function as mother wavelet. Localization of signal characteristics in time and frequency domains can be accomplished with this wavelet function. Figure 1 shows the wavelet spectra of horizontal component of geomagnetic field variations over Tirunelveli (8.7°N, 77.8°E) and *F* region peak critical frequency (f_oF_2) obtained from the GPS radio occultation measurements of COSMIC satellites at 7.5°N. The cone of influence is shown as crossed lines, where (light shaded area) edge effects are important. The wavelet analysis of the horizontal component of geomagnetic field variations shows periodicities near 3 days. These periodicities are dominantly observed during the day numbers 30–40. It is remarkable that f_oF_2 also shows similar periodicities during the day numbers 30–40. Though there are other periodicities also present, it may be noted that only 2–4 day periodicity is present simultaneously in the both parameters. However, the 2–4 day periodicity is not observed in *F* region peak height (h_mF_2) (not shown). As these periodicities appear to be those of commonly observed planetary waves in the mesospheric winds, the horizontal winds over Tirunelveli (8.7°N, 77.8°E) are subjected to wavelet analysis to infer whether similar periodicities are present in the winds.

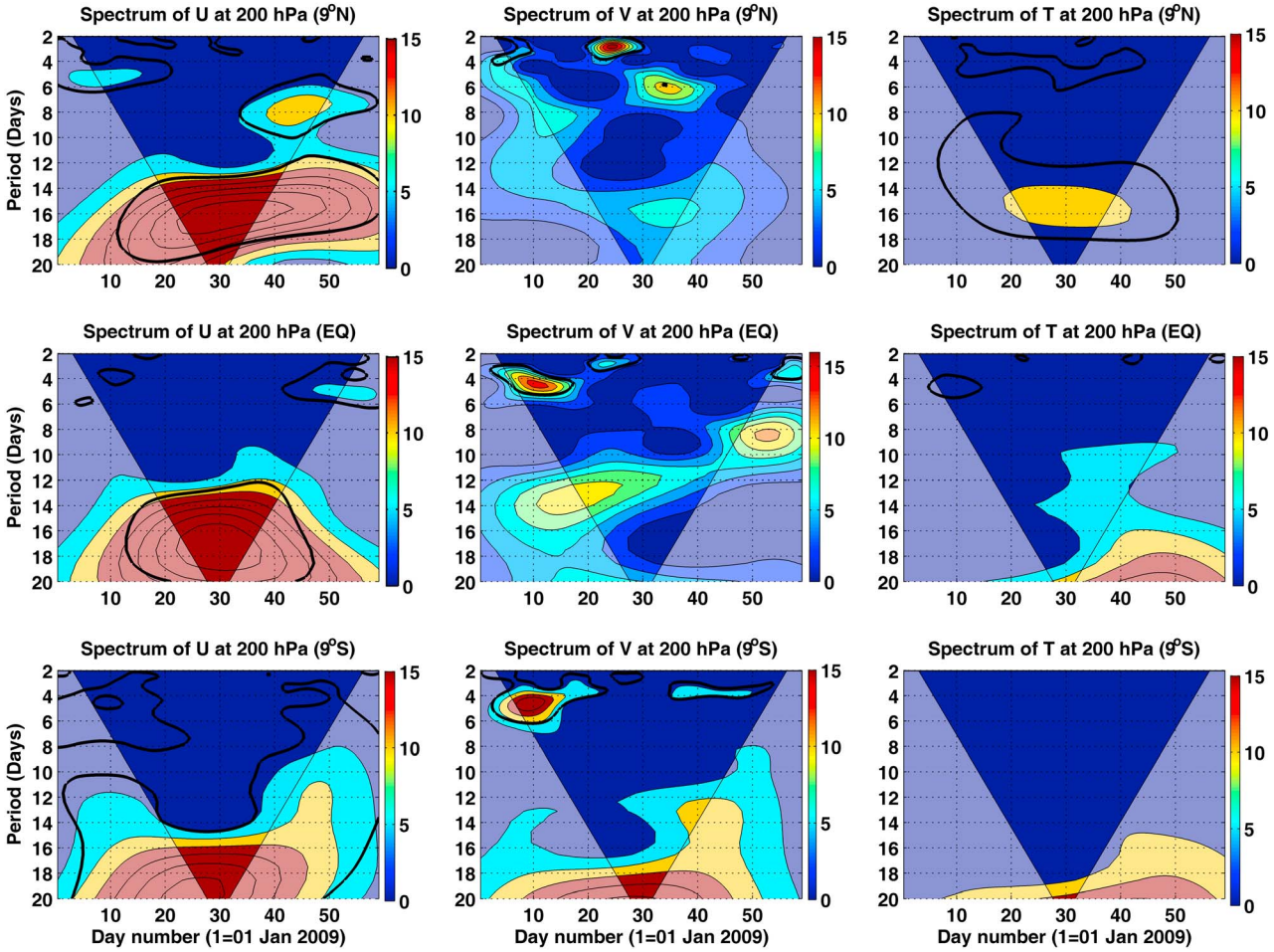

Figure 4. Wavelet spectrum of ERA-Interim zonal mean zonal wind, meridional wind, and temperature at 200 hPa at (top) 9°N, (middle) the equator, and (bottom) 9°S.

The wavelet spectrum shown in Figure 2 clearly indicates the presence of the ∼2–4 day wave in meridional winds during the day numbers 20–30, which include a major SSW event, as noted at stratospheric heights. As the enhancement of 2–4 day wave is observed during the period, when a major SSW event occurred at high-latitude stratosphere, it is investigated whether there is any relation between the wave activity and the SSW event. The breaking of polar vortex associated with the occurrence of SSW events produce intrusions of stratospheric air with high potential vorticity (PV) into the tropical upper troposphere [*Waugh and Polvani*, 2000]. The longitude-time of PV maps shown in Figure 3 reveals that the intrusions of high PV occur prior to the occurrence of SSW in the longitude region east of 220°E. *Waugh and Polvani* [2000] studied climatology of PV intrusions and noted that wave breaking events that transport high PV air directly into the deep tropics occur predominantly during northern winter, when eastward winds prevail over the equator with more frequent events in the Pacific region (180°–260°E). However, on the day of peak warming (23 January 2009), the PV intrusion can be observed more at longitudes near 60°E, in addition to the one near east of 200°E. PV intrusions precede occurrences of deep convection in the downstream side, as they have a less stable potential temperature distribution within and immediately below. The decrease in the static stability can trigger vertical motions and deep convection. The latent heat release due to deep convection is an importance source mechanism for the equatorial wave disturbances. It may be noted that equatorial waves can be amplified, if the midlatitude disturbances propagate intermittently toward the equator in the form of potential vorticity intrusion [*Hayashi and Golder*, 1978]. Figure 4 shows wavelet spectrum of zonal mean zonal wind, meridional wind and temperature at 200 hPa at 9°N, the equator and 9°S. The ∼2–4 day periodicities are clearly evident in meridional wind during the day numbers 20–30, when a major SSW event occurs. The ∼2–4 day wave is more dominant at 9°N, weaker at the equator and not present at 9°S. The wave does not seem to be an ultrafast Kelvin wave reported at mesospheric heights, as the wave is dominant in meridional winds. The wave is observed at latitudes up to 27°N (not shown). In addition, there are other periodicities in meridional winds near 6 days during the day numbers 30 and 40 only at 9°N, 4–6 day periodicities at both the equator and 9°S. In order to find the horizontal characteristics of 2–4 day wave, time-longitude plots of 2–4 day filtered zonal wind, meridional wind and temperature are shown in Figure 5. It is clearly evident that the wave is an eastward

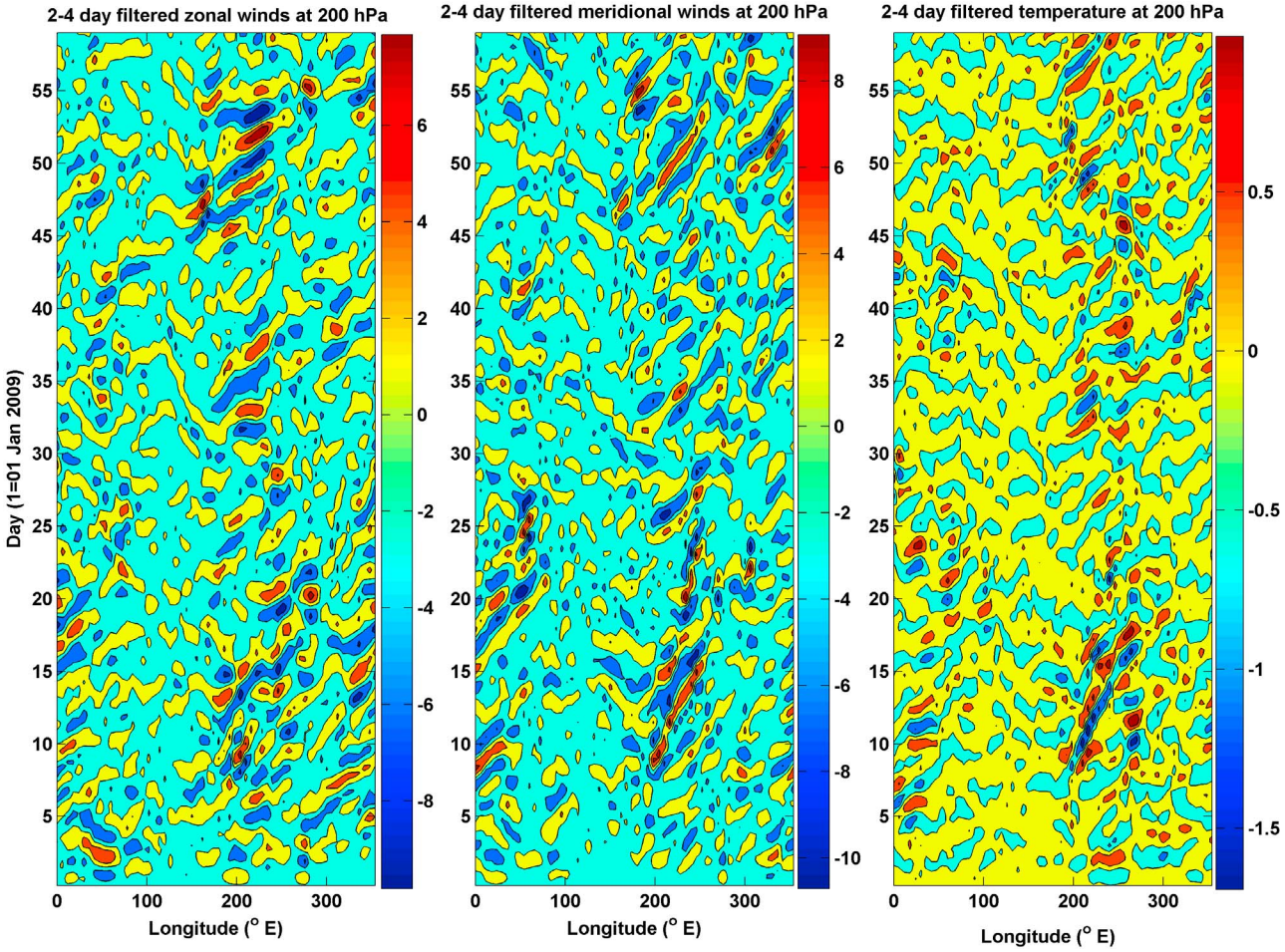

Figure 5. The 2–4 day filtered ERA-Interim zonal wind, meridional wind, and temperature at 200 hPa over the equator.

propagating wave with horizontal wavelength of nearly ~6500 km indicating that the wave has zonal wave number 6. Large wave activity is observed only in limited longitudes around 200°–250°E and 0–50°E indicating that the wave is not a planetary wave and is mostly of inertia-gravity wave type. In particular, the wave activity is stronger over the central and eastern Pacific both before and during the SSW event and over Indian sector during the SSW event only. *Waugh and Funatsu* [2003] showed that deep convection mostly occurs at the downstream side of the PV intrusions. In order to see whether 2–4 day periodicity is present in OLR, a proxy for tropical convection, the daily interpolated OLR is subjected to wavelet analysis and the spectrum is shown in Figure 6a. It clearly indicates the presence of 2–4 day periodicity during the day numbers 30–40. The periodicity appears significantly in OLR with a delay of nearly 10 days after its appearance in the meridional winds at 200 hPa (Figure 4). The delay could be due to time taken by the equatorial convection to respond to the lateral forcing. It indicates that the periodicity in the OLR might be induced by the propagation of midlatitude disturbances toward the equator. *Lamb* [1973] suggested that the tropical atmosphere selectively responds to lateral forcing generating equatorial wave disturbances with characteristics similar to those of the observed mixed Rossby-gravity wave and the gravest Rossby wave.

[10] The 2–4 day filtered OLR (Figure 6b) show that the wave is significantly present in OLR in the longitude region west of 200°E and east of 300°E indicating that the wave is not generated owing to equatorial convection. The enhancement of the ~2 day wave in the longitude bands clearly reveals that the wave may have been generated by the intrusion of potential vorticity. The wave may propagate to upper heights and cause significant variabilities in the mesosphere-thermosphere-ionosphere system.

[11] To obtain vertical wavelength of the ~2–4 day wave, the daily radiosonde winds and temperature observations (up to 30 km) and Rayleigh lidar temperature observations (25–70 km) and MF radar winds at Tirunelveli are subjected to the 2–4 day band-pass filter and from the phase variation with height, vertical wavelength of the wave is estimated. The vertical wavelength of the wave is around 4 km in the radiosonde winds (Figure 7c) and Rayleigh lidar temperature (Figure 7d). However, it increases to 12–15 km in the MF radar winds (Figures 7e–7f).

[12] However, during the day numbers 27–30, no phase variation with height is noticed in the Rayleigh lidar temperature (Figure 7d). The phase of the wave shows little

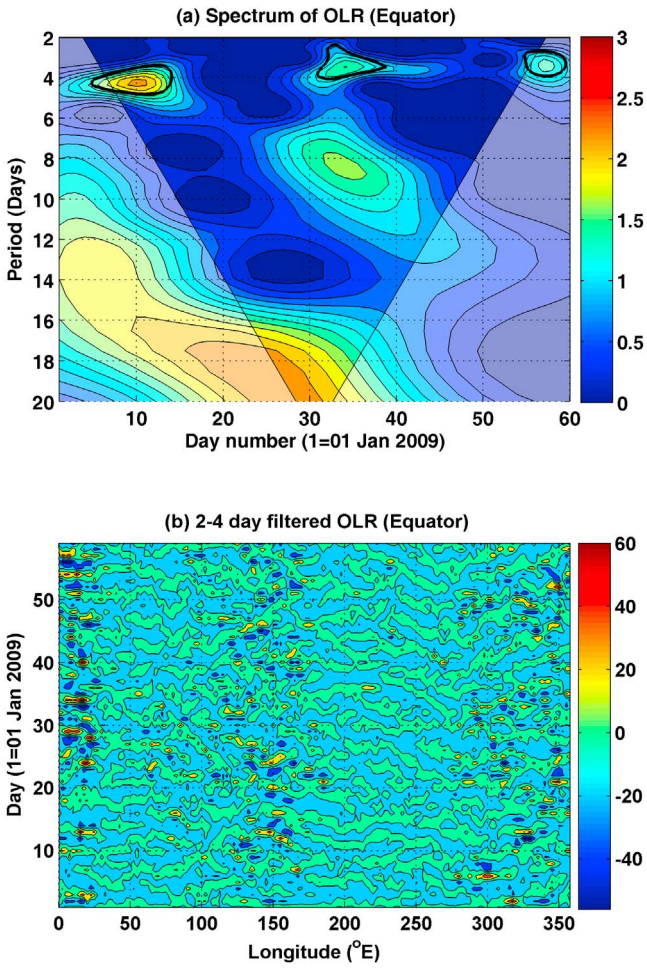

Figure 6. (a) Wavelet spectrum of the zonal mean OLR at the equator and (b) longitude-time cross section of the 2–4 day filtered zonal mean OLR.

variation with height and is consistent with the results of *Deepa et al.* [2007], who earlier noted a ~4 day wave with little phase variation with height in rocketsonde wind measurements at Sriharikota (13.7°N, 80.2°E). *Takahashi et al.* [2005] observed quasi–2 and 4 day period oscillations in the ionospheric *F* layer bottom height and airglow emission intensity and they, however, could not identify the type and origin of these waves.

4. Discussion and Conclusion

[13] We have observed a strong 2–4 day wave activity in the COSMIC *F* region peak frequency (f_oF_2), which is related to peak electron density at 7.5°N and horizontal component of geomagnetic field variations over Tirunelveli during the SSW event of 2009. Similar wave is observed strongly in the mesospheric meridional winds observed by MF radar at Tirunelveli. The ERA observations at 9°N and the equator shows clearly the eastward propagating 2–4 day wave in the central and eastern Pacific before and during the SSW event and over Indian sector during the SSW event only. It may be noted that the wavelet spectrum of OLR at the equator show the presence of ~3 day wave during the day numbers 30–60 and the wave is absent away from the equator indicating that the wave appears to be an equatorially trapped wave. Though the equatorial convective heating is an important excitation mechanism of the equatorially trapped waves, lateral forcing and wave-CISK (conditional instability of the second kind) have also been suggested for the excitation of these waves [*Magana and Yanai*, 1995].

[14] It may be noted that in the present work, 2–4 day wave is present in the ERA winds and temperature at 200 hPa in the longitude band around 50°E during the SSW event and 200–250°E before and during the SSW event. The appearance of these waves up to 27°N indicates that it is an extratropical disturbance and it cannot be considered as an equatorial wave. Besides, the wave is observed in ERA meridional winds prior to that observed in OLR. It may be noted that the PV intrusions shown for different days for January 2009 reveal that the intrusion occurs in the longitude band 200–250°E before the SSW event and an additional; however, stronger intrusion is in the longitude around 50°E during SSW event. *Waugh and Funatsu* [2003] identified that deep intrusions always precede occurrences of deep convection in the tropical eastern Pacific. *Hoskins and Yang* [2000] showed that the equatorial response to high-latitude forcing is due to a direct projection of the forcing onto equatorially trapped waves and the Rossby-gravity wave dominates for the ~4 day period forcing and Rossby waves are found for the ~8 day period forcing. According to them, the presence of equatorial eastward winds may not be necessary for the propagating of high-latitude PV forcing to the equator. As suggested by *Lamb* [1973], the tropical atmosphere selectively responds to lateral forcing generating equatorial wave disturbances with wave numbers and frequencies similar to those of the observed MRGW and the gravest Rossby wave. In her theory, these waves are then enhanced by the effect of condensational heating. By general circulation model (GCM) experiments, *Hayashi and Golder* [1978] showed that equatorial waves can be excited owing to convective heating even if midlatitude disturbances are eliminated. However, these waves are significantly enhanced if midlatitude disturbances propagate intermittently toward the equator. An eastward moving ~4 day wave is a characteristic feature of polar winter stratosphere.

[15] *Mizuta and Yoden* [2002] observed an eastward propagating wave with period near 4 days in some years in the polar region during midwinter, even though polar vortex is not disturbed. They related isentropic mixing inside the polar vortex with the amplitude of the 4 day wave and its interannual variability. The 4 day wave is a planetary-scale phenomenon with zonal wave numbers (k) of 1–4, and propagates eastward with approximately the same phase speed such that the k = 1 wave has a period of near 4 days, while the k = 2 wave has a period of near 2 days. Barotropic instability in the poleward flank of the stratospheric polar jet or combined barotropic and baroclinic instabilities associated with the double-jet structure of mesospheric eastward winds have been suggested as the source mechanisms for these waves [*Hartmann*, 1983; *Manney*, 1991]. The GCM model results of *Watanabe et al.* [2009] could show amplification of the 4 day wave having similar character with that observed at polar stratosphere, developed in association with the successfully simulated mesospheric instabilities of the mean flow. However, our observations show that the zonal

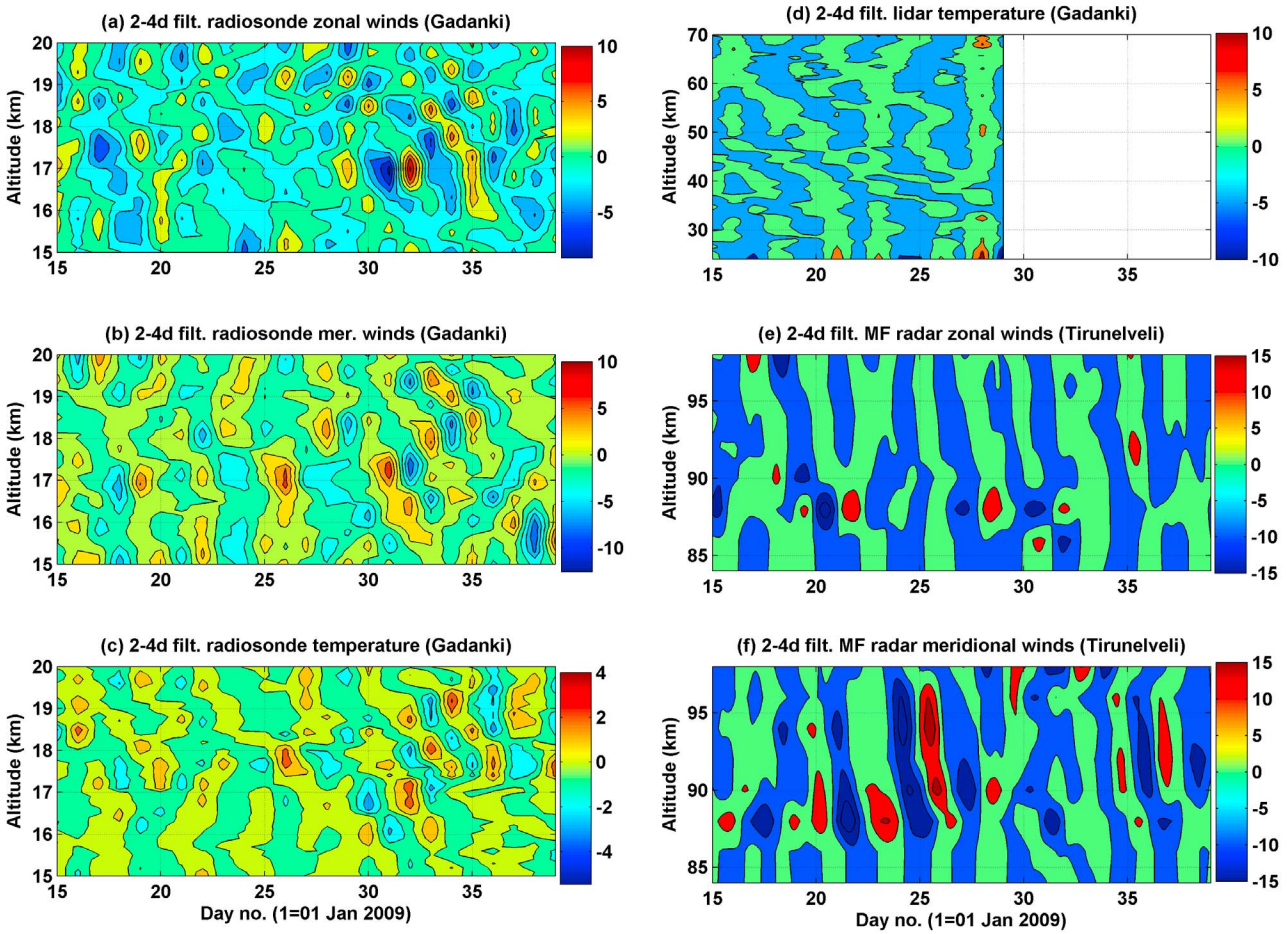

Figure 7. (a–c) The 2–4 day filtered radiosonde zonal and meridional winds and temperature over Gadanki, (d) Rayleigh lidar temperature over Gadanki, and (e and f) MF radar zonal and meridional winds over Tirunelveli.

wave number of 2–4 day wave is 6. Besides, the ~4 day wave cannot be observed in the ERA winds and temperature at high-latitude stratosphere during January 2009. It indicates that the 4 day wave, which has commonly been observed in the high-latitude stratosphere, is different from the wave observed in the present study.

[16] Model results from *Liu et al.* [2010] suggest that although the quasi-stationary planetary wave does not propagate deep into the ionosphere or to low latitudes owing to the presence of critical layers and strong molecular dissipation, the planetary wave and tidal interaction leads to large changes in tides, which can strongly impact the ionosphere at low and middle latitudes through the E region wind dynamo. In the present study, the diurnal tidal amplitude in meridional winds at upper mesospheric heights over Tirunelveli (8.7°N, 77.8°E) does not show any significant periodicity near ~2–4 days. There is an indication of 2–4 day modulation of diurnal tide in zonal winds during the day numbers 20–25 (not shown) and it reveals the occurrence of nonlinear interaction between tides and inertia-gravity wave. Large zonal gradients of zonal and meridional winds from the tidal components and the zonal gradient of electric conductivities at dawn can produce large convergence/divergence of Hall and Pedersen currents, which in turn produces a polarization electric field. The ionospheric changes are dependent on both the longitude and local time, and are determined by the amplitudes and phases of the superposing wave components. However, in the present work, there is a delay between the occurrence of the nonlinear interaction and periodicities observed in geomagnetic field and in f_oF_2. Hence, it is also possible that the 2–4 day wave in meridional winds could reach to at least *E* region heights and modulate the current system directly.

[17] **Acknowledgment.** Robert Lysak thanks the reviewers for their assistance in evaluating this paper.

References

Altadill, D., and E. M. Apostolov (2001), Vertical propagating signatures of wave-type oscillations (2 and 6.5 days) in the ionosphere obtained from electron-density profiles, *J. Atmos. Terr. Phys.*, *63*, 823–834, doi:10.1016/S1364-6826(00)00199-1.

Charney, J. G. (1963), A note on large-scale motions in the tropics, *J. Atmos. Sci.*, *20*, 607–609, doi:10.1175/1520-0469(1963)020<0607:ANOLSM>2.0.CO;2.

Chau, J. L., B. G. Fejer, and L. P. Goncharenko (2009), Quiet variability of equatorial **E** × **B** drifts during a sudden stratospheric warming event, *Geophys. Res. Lett.*, *36*, L05101, doi:10.1029/2008GL036785.

Chen, P.-R. (1992), Two-day oscillation of the equatorial ionization anomaly, *J. Geophys. Res.*, *97*, 6343–6357, doi:10.1029/91JA02445.

Daubechies, I. (1992), *Ten Lectures on Wavelets*, 357 pp., Soc. for Ind. and Appl. Math., Univ. Sci. Cent, Philadelphia, Pa.

Debashis Nath, M. V. Ratnam, V. V. M. J. Rao, B. V. K. Murthy, and S. Vijaya Bhaskara Rao (2009), Gravity wave characteristics observed over a tropical station using high-resolution GPS radiosonde soundings, *J. Geophys. Res.*, *114*, D06117, doi:10.1029/2008JD011056.

Deepa, V., G. Ramkumar, and K. K. Kumar (2007), Observational evidence for the generation of a 4-day oscillation in the low-latitude middle atmosphere associated with an anomalous stratospheric cooling, *Ann. Geophys.*, *25*, 1959–1965, doi:10.5194/angeo-25-1959-2007.

Fagundes, P. R., V. G. Pillat, M. J. A. Bolzan, Y. Sahai, F. Becker-Guedes, J. R. Abalde, S. L. Aranha, and J. A. Bittencourt (2005), Observations of *F* layer electron density profiles modulated by planetary wave type oscillations in the equatorial ionospheric anomaly region, *J. Geophys. Res.*, *110*, A12302, doi:10.1029/2005JA011115.

Goncharenko, L., and S. R. Zhang (2008), Ionospheric signatures of sudden stratospheric warming: Ion temperature at middle latitude, *Geophys. Res. Lett.*, *35*, L21103, doi:10.1029/2008GL035684.

Hartmann, D. L. (1983), Barotropic instability of the polar night jet stream, *J. Atmos. Sci.*, *40*, 817–835, doi:10.1175/1520-0469(1983)040<0817:BIOTPN>2.0.CO;2.

Hauchecorne, A., and M. L. Chanin (1980), Density and temperature profiles obtained by lidar between 35 and 70 km, *Geophys. Res. Lett.*, *7*, 565–568, doi:10.1029/GL007i008p00565.

Hayashi, Y., and D. G. Golder (1978), The generation of equatorial transient planetary waves: Control experiments with a GFDL general circulation model, *J. Atmos. Sci.*, *35*, 2068–2082, doi:10.1175/1520-0469(1978)035<2068:TGOETP>2.0.CO;2.

Hoskins, B. J., and G.-Y. Yang (2000), The equatorial response to high latitude forcing, *J. Atmos. Sci.*, *57*, 1197–1213, doi:10.1175/1520-0469(2000)057<1197:TERTHL>2.0.CO;2.

Lamb, V. R. (1973), The response of the tropical atmosphere to mid-latitude forcing, Ph.D. thesis, 151 pp., Univ. of Calif., Los Angeles.

Laštovička, J., and D. Pancheva (1991), Changes in the characteristics of planetary waves at 80–100 km over central and southern Europe since 1980, *Adv. Space Res.*, *11*, 31–34, doi:10.1016/0273-1177(91)90399-5.

Lau, K. M., and P. H. Chan (1983), Short-term climate variability and atmospheric teleconnections from satellite-observed outgoing longwave radiation. I: Simultaneous relationships, *J. Atmos. Sci.*, *40*, 2735–2750, doi:10.1175/1520-0469(1983)040<2735:STCVAA>2.0.CO;2.

Liu, H. L., W. Wang, A. D. Richmond, and R. G. Roble (2010), Ionospheric variability due to planetary waves and tides for solar minimum conditions, *J. Geophys. Res.*, *115*, A00G01, doi:10.1029/2009JA015188.

Magana, V., and M. Yanai (1995), Mixed Rossby-gravity waves triggered by lateral forcing, *J. Atmos. Sci.*, *52*, 1473–1486, doi:10.1175/1520-0469(1995)052<1473:MRWTBL>2.0.CO;2.

Manney, G. L. (1991), The stratospheric 4-day wave in NMC data, *J. Atmos. Sci.*, *48*, 1798–1811, doi:10.1175/1520-0469(1991)048<1798:TSDWIN>2.0.CO;2.

Matsuno, T. (1971), A dynamical model of the stratospheric sudden warming, *J. Atmos. Sci.*, *28*, 1479–1494, doi:10.1175/1520-0469(1971)028<1479:ADMOTS>2.0.CO;2.

Mizuta, R., and S. Yoden (2002), Interannual variability of the 4-day wave and isentropic mixing inside the polar vortex in midwinter of the Southern Hemisphere upper stratosphere, *J. Geophys. Res.*, *107*(D24), 4798, doi:10.1029/2001JD002037.

Munro, G. H. (1948), Short-period changes in the *F* region of the ionosphere, *Nature*, *162*, 886–887, doi:10.1038/162886a0.

Rajaram, R., and S. Gurubaran (1998), Seasonal variabilities of low-latitude mesospheric winds, *Ann. Geophys.*, *16*, 197–204, doi:10.1007/s00585-998-0197-4.

Rishbeth, H., and M. Mendillo (2001), Patterns of F_2 layer variability, *J. Atmos. Sol. Terr. Phys.*, *63*, 1661–1680, doi:10.1016/S1364-6826(01)00036-0.

Rocken, C., Y.-H. Kuo, W. Schreiner, D. Hunt, S. Sokolovskiy, and C. McCormick (2000), COSMIC system description, *Terr. Atmos. Oceanic Sci.*, *11*, 21–52.

Schreiner, W., C. Rocken, S. Sokolovskiy, S. Syndergaard, and D. Hunt (2007), Estimates of the precision of GPS radio occultations from the COSMIC/FORMOSAT-3 mission, *Geophys. Res. Lett.*, *34*, L04808, doi:10.1029/2006GL027557.

Takahashi, H., L. M. Lima, C. M. Wrasse, M. A. Abdu, I. S. Batista, D. Gobbi, R. A. Buriti, and P. P. Batista (2005), Evidence on 2–4 day oscillations of the equatorial ionosphere h′F and mesospheric airglow emissions, *Geophys. Res. Lett.*, *32*, L12102, doi:10.1029/2004GL022318.

Tsuda, T., M. Venkat Ratnam, T. Kozu, and S. Mori (2006), Characteristics of 10 day Kelvin wave observed with radiosondes and CHAMP/GPS occultation during the CPEA campaign (April–May 2004), *J. Meteorol. Soc. Jpn.*, *84A*, 277–293, doi:10.2151/jmsj.84A.277.

Uppala, S. M., et al. (2005), The ERA-40 Re-Analysis, *Q. J. R. Meteorol. Soc.*, *131*, 2961–3012, doi:10.1256/qj.04.176.

Watanabe, S., Y. Tomikawa, K. Sato, Y. Kawatani, K. Miyazaki, and M. Takahashi (2009), Simulation of the eastward 4-day wave in the Antarctic winter mesosphere using a gravity wave resolving general circulation model, *J. Geophys. Res.*, *114*, D16111, doi:10.1029/2008JD011636.

Waugh, D. W., and B. M. Funatsu (2003), Intrusions in to the tropical atmosphere: Three-dimensional structure and accompanying ozone and OLR distributions, *J. Atmos. Sci.*, *60*, 637–653, doi:10.1175/1520-0469(2003)060<0637:IITTUT>2.0.CO;2.

Waugh, D. W., and L. M. Polvani (2000), Climatology of intrusions into the tropical upper troposphere, *Geophys. Res. Lett.*, *27*, 3857–3860, doi:10.1029/2000GL012250.

Webster, P. J., and J. R. Holton (1982), Cross-equatorial response to middle-latitude forcing in a zonally varying basic state, *J. Atmos. Sci.*, *39*, 722–733, doi:10.1175/1520-0469(1982)039<0722:CERTML>2.0.CO;2.

Xiong, J., W. Wan, B. Ning, L. Liu, and Y. Gao (2006), Planetary wave type oscillations in the ionosphere and their relationship to mesospheric/lower thermospheric and geomagnetic disturbances at Wuhan (30.61°N, 114.51°E), *J. Atmos. Sol. Terr. Phys.*, *68*, 498–508, doi:10.1016/j.jastp.2005.03.018.

S. Sathishkumar, Equatorial Geophysical Research Laboratory, Indian Institute of Geomagnetism, Krishnapuram, Tirunelveli 627 011, India.

S. Sridharan, National Atmospheric Research Laboratory, Pakala Mandal, Chittoor, Gadanki 517 112, India. (susridharan@narl.gov.in)